

A novel analytical solution for ponded infiltration with consideration of a developing saturated zone

DongHao Ma¹, Zhipeng Liu², SiCong Wu¹, and Jiabao zhang¹

¹Institute of Soil Science, Chinese Academy of Sciences

²Institute of Soil and Water Conservation, Chinese Academy of Sciences & Ministry of Water Resources

December 22, 2022

Abstract

Ponding at the soil surface exerts profound impacts on infiltration. However, the effects of ponding depth on infiltration, especially the development of a saturated zone below the soil surface, have not been considered in present infiltration models. A new general Green-Ampt model solution (GAMS) was derived for a one-dimensional vertical infiltration into soils under a uniform initial moisture distribution with ponding on its surface. An expression was included in the new solution for simulating the saturated layer developed below the soil surface as long as the pressure head at the surface is greater than the water-entry suction. The GAMS simulates the infiltration processes closer to the numerical solution by HYDRUS-1D than the traditional and a recently improved Green-Ampt model. Moreover, an inversion method to improve the estimates of soil hydraulic parameters from one-dimensional vertical infiltration experiments that is based on the GAMS was suggested. The effect of ponding depth (hp), initial soil moisture content, soil texture, and hydraulic soil properties (Ks, hd and n) in the saturated zone was also evaluated. The results indicate that the saturated zone developed at a much faster rate than the unsaturated zone during infiltration. Generally, a larger saturated zone was found for soils with higher initial soil moisture content, coarser texture, higher Ks values and lower hd and n. Our findings reveal that including the saturated zone in the infiltration model yields a better estimate for the soil hydraulic parameters. The proposed GAMS model can improve irrigation design and rainfall-runoff simulations.

Hosted file

951103_0_art_file_10492678_rm7hnn.docx available at <https://authorea.com/users/568938/articles/614562-a-novel-analytical-solution-for-ponded-infiltration-with-consideration-of-a-developing-saturated-zone>

1
2 **A novel analytical solution for ponded infiltration with consideration of a developing**
3 **saturated zone**
4

5 **DongHao Ma^{1#}, ZhiPeng Liu^{2#}, SiCong Wu^{1,3}, and JiaBao Zhang¹**

6 ¹ State Experimental Station of Agro-Ecosystem in Fengqiu, State Key Laboratory of Soil and
7 Sustainable Agriculture, Institute of Soil Science, Chinese Academy of Sciences, Nanjing
8 210008, China.

9 ² College of Resources and Environmental Sciences, Nanjing Agricultural University, Nanjing
10 210095, China.

11 ³ University of Chinese Academy of Sciences, Beijing 100049, China.

12 ³ University of Chinese Academy of Sciences, Beijing 100049, China.

13 [#] These authors contributed equally to this work.

14 Corresponding author: JiaBao Zhang (jbzhang@issas.ac.cn)
15

16 **Key Points:**

- 17
- The saturated zone is longer than the unsaturated wetted zone during ponded infiltration.
 - The new proposed infiltration equation includes an expression of the saturation zone versus time.
 - The new solution simulates infiltration and estimates soil hydraulic properties more accurately.
- 21

22 **Abstract**

23 Ponding at the soil surface exerts profound impacts on infiltration. However, the effects
24 of ponding depth on infiltration, especially the development of a saturated zone below the soil
25 surface, have not been considered in present infiltration models. A new general Green-Ampt
26 model solution (GAMS) was derived for a one-dimensional vertical infiltration into soils under a
27 uniform initial moisture distribution with ponding on its surface. An expression was included in
28 the new solution for simulating the saturated layer developed below the soil surface as long as
29 the pressure head at the surface is greater than the water-entry suction. The GAMS simulates the
30 infiltration processes closer to the numerical solution by HYDRUS-1D than the traditional and a
31 recently improved Green-Ampt model. Moreover, an inversion method to improve the estimates
32 of soil hydraulic parameters from one-dimensional vertical infiltration experiments that is based
33 on the GAMS was suggested. The effect of ponding depth (h_p), initial soil moisture content, soil
34 texture, and hydraulic soil properties (K_s , h_d and n) in the saturated zone was also evaluated. The
35 results indicate that the saturated zone developed at a much faster rate than the unsaturated zone
36 during infiltration. Generally, a larger saturated zone was found for soils with higher initial soil
37 moisture content, coarser texture, higher K_s values and lower h_d and n . Our findings reveal that
38 including the saturated zone in the infiltration model yields a better estimate for the soil
39 hydraulic parameters. The proposed GAMS model can improve irrigation design and rainfall-
40 runoff simulations.

41 **1 Introduction**

42 Infiltration is one of the most important components of land surface water cycles. Accurate
43 simulation of infiltration rate is crucial in hydrological forecast, biogeochemical process
44 simulation, agricultural water management, and soil and water conversation ([Assouline, 2013](#)).

45 However, infiltration is a complex process affected by many factors such as (1) soil structure and
46 its spatial heterogeneity influenced by soil mineral particles and organic matter in physical,
47 chemical and biological cycles (Bonetti et al., 2021; Fatichi et al., 2020; Vereecken et al., 2022);
48 (2) chemical compositions of the soil water and infiltrating water (Klopp and Daigh, 2020); (3)
49 initial soil moisture distribution across soil profile (Stewart et al., 2013; Wu et al., 2021); (4) type
50 and rate of water supply on the soil surface (Assouline et al., 2007; Corradini et al., 1994; 1997).
51 During the past one century, a vast amount of attentions have been attracted to the studies on
52 developing mathematical infiltration models under various conditions (Green and Ampt, 1911;
53 Haverkamp et al., 1994; Hogarth et al., 2013; Morbidelli et al., 2018; Moret-Fernández et al.,
54 2020; Parlange, 1971; Parlange et al., 1982; Philip, 1969; Selker and Assouline, 2017; Stewart,
55 2019; Talsma and Parlange, 1972), as well as establishing methods to determine infiltration
56 model parameters (Angulo-Jaramillo et al., 2019; Ma et al., 2017; Neuman, 1976; Parlange,
57 1975; Touma et al., 2007; Valiantzas, 2010; Vauclin and Haverkamp, 1985). Generally, the
58 model expression and its deriving method for one-dimensional infiltration into homogeneous
59 soils with uniform initial soil moisture distributions under a saturated or ponded upper boundary
60 condition were taken as a base for the development of one, two or three-dimensional infiltration
61 models under more complex conditions (Kargas and Londra, 2021; Selker and Assouline, 2017;
62 Wu et al., 2022).

63 The effects of ponding on infiltration can be profound (Philip, 1958a; 1958b), especially in
64 initially wet soils, and it acts through not only added surface water pressure but also water
65 redistribution in soils (Parlange, 1972). The ponding can increase water pressure at soil surface
66 and thus improve infiltration. Soil moisture profile would change accordingly to transmit and
67 redistribute soil water potential gradient across the whole profile. Consequently, a saturated zone

68 forms below the soil surface and increases during ponded infiltration. In addition, for soils with
69 non-zero water-entry suction ($-h_d$), the saturated zone, defined as tension-saturated zone by
70 (Philip, 1958a), would still develop even if the surface water pressure is zero or a negative value
71 greater than water-entry suction (Haverkamp et al., 1990). Given that soils with non-zero water-
72 entry suction are common in nature, a saturated zone composed of the two types above was
73 found in most soil moisture profiles during infiltration under a surface pressure greater than
74 water-entry suction (Philip, 1958a).

75 However, the effects of ponded water on infiltration have not been fully considered in the
76 two types of widely used infiltration models under ponded conditions. One type includes the
77 empirical and semi-empirical models which neglect the effect of ponding depth, such as Horton's
78 infiltration model (Horton, 1941) in hydrology, Kostiakov model (Kostiakov, 1932) and Lewis-
79 Kostiakov model (Mezencev, 1948) in surface irrigation. The other type includes analytical and
80 semi-analytical infiltration models, such as Philip's Two-Term model (Philip, 1957a),
81 Brutsaert's model (Brutsaert, 1977), Parlange's three-parameter model (Parlange et al., 1982),
82 Swartzendruber model (Swartzendruber, 1987), the traditional Green-Ampt model (TGAM)
83 (Green and Ampt, 1911) and the recently improved Green-Ampt model (GAME) (Ma et al.,
84 2015). In these analytical and semi-analytical models, the effects of ponding depth on infiltration
85 were only expressed in the form of an added surface pressure head.

86 Actually in 1958, Philip (1958a) has proposed an analytical method which includes a series
87 expression of the time-dependent saturated zone by assuming a negligible effect of ponding
88 depth on infiltration rate. His solution showed a good simulation accuracy in a short time and
89 revealed a time-dependent soil moisture profile shape (Philip, 1958b). In 1972, Parlange (1972)
90 built a general iterative solution in integral forms addressing the infiltration under ponded

91 conditions, which can achieve accurate simulation for a longer time. A more concise solution
92 was derived by [Haverkamp et al. \(1990\)](#) to depict the effects of ponding depth on infiltration,
93 based on the first-order approximation of the above Parlange's solution ([Parlange, 1972](#)) and a
94 flux-saturation relation. These solutions substantially improved the infiltration simulation by
95 taking into account the profound effects of ponding depth on infiltration. Unfortunately, few of
96 the results has been adopted in subsequent infiltration simulations. One of the most important
97 reasons is that the solutions in integral forms are too complex to use in practice.

98 The main applications of infiltration formulas are to simulate infiltration and to estimate its
99 parameters. During the past two decades, some analytical or semi-analytical solutions to
100 infiltration problems have found their exciting function of rapidly inverting soil hydraulic
101 properties from infiltration experiments ([Jaiswal et al., 2022](#); [Ma et al., 2016, 2017](#); [Rahmati et](#)
102 [al., 2021](#)) and overcoming the problem of non-convergence and unitability in numerical
103 inversion. However, the accuracy of the inverted parameters of soil hydraulic property model
104 were found sensitive to the accuracy of the forward analytical or semi-analytical solutions ([Ma et](#)
105 [al., 2009](#)). A small difference in an infiltration formula from a real infiltration process may result
106 in time-dependent estimated parameters in its applications. Our previous studies ([Ma et al., 2015,](#)
107 [2017](#)) exhibited that to build the quantitative relationship between the Green-Ampt model simple
108 in form and Richards equation accurate in simulation was an effective approach to achieve soil
109 hydraulic properties from infiltration experiments. The traditional Green-Ampt model (TGAM)
110 is just a special solution to Richards equation for soils with delta-type diffusivity ([Philip, 1957b](#))
111 and thus too simplified to accurately estimate soil hydraulic properties. Recently, a more
112 sophisticated Green-Ampt model (GAME) found its deterministic relevance to Richards equation
113 for general soils ([Ma et al., 2015](#)). Based on the new approximate analytical solution, a

114 compatible method was derived to determine soil hydraulic properties (Ma et al., 2015, 2017).
 115 However, the effects of ponding depth on infiltration were still not fully considered in that
 116 solution, especially the changes in the shape of soil moisture profile.

117 Therefore, the objectives of this research are (1) to develop a new solution to one-
 118 dimensional infiltration under ponded conditions, including a simple infiltration equation with
 119 ponding depth effects and explicit expressions of saturated and unsaturated zone length varying
 120 with time; (2) to evaluate the effects of ponding depth on infiltration simulation and soil
 121 hydraulic parameter estimation.

122 2 Theory

123 2.1 A general solution to infiltration with a constant water head

124 According to Ma et al. (2015), a general relationship for a vertical infiltration into soils with
 125 initially uniform soil moisture distribution under ponding with a constant water depth is given as:

$$126 \int_0^{z_f} ((J_{w0} - K_i) F + K_i) dz = \int_0^{z_f} K dz - \int_0^{h_i} K dh - \int_{h_p}^0 K dh \quad (1)$$

127 where K is the soil hydraulic conductivity (cm min^{-1}); K_i is the soil hydraulic conductivity at the
 128 initial soil water content (cm min^{-1}); J_{w0} is the infiltration rate or surface soil water flux (cm min^{-1});
 129 F is the soil water flux-saturation function; h is the soil water pressure head (cm); h_i is the
 130 initial soil water pressure head (cm); h_p is the water depth on soil surface (cm); z is the soil depth
 131 (cm) with zero point at soil surface and downward coordinate axis; and z_f is the wetting front
 132 advance or the length of wetted zone (cm).

133 Since J_{w0} is a variable independent of z , after rearranging Equation (1), it is expressed as:

134

$$J_{w0} = \frac{\int_0^{z_f} (K - (1-F)K_i) dz - \int_0^{h_i} K dh - \int_{h_p}^0 K dh}{\int_0^{z_f} F dz} \quad (2)$$

135

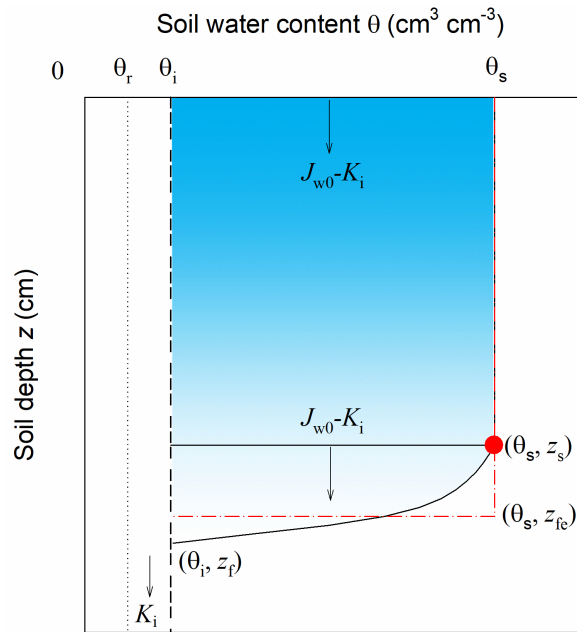
136

137

138

139

Since the saturated soil drains only when water head drops below air entry suction $-h_d$ (cm), there must be a saturated zone on the upper part of the wetted zone where $h > -h_d$. Assuming that soil water content profile in the unsaturated wetted zone can be described with a simple function (e.g. in Ma et al., 2015) and its relative shape does not change with time, then the soil water content profile (Figure 1) can be described as:



140

141

142

143

144

145

146

Figure 1. Schematic diagram of soil moisture profile including saturated and unsaturated wetted zones. θ_r and θ_i are the residual and initial soil water content, respectively; θ_s is the soil water content at the water inlet; J_{w0} is the surface water flux; K_i is the soil hydraulic conductivity at θ_i ; z_s is the length of saturated zone; z_f and z_{fe} are actual and equivalent lengths of wetted zone, respectively.

147
$$S = \frac{\theta - \theta_r}{\theta_s - \theta_r} = \begin{cases} 1 & z < z_s \\ S \left(\frac{z - z_s}{z_f - z_s} \right) & z_f \geq z \geq z_s \\ S_i & z \geq z_f \end{cases} \quad (3)$$

148 where θ is the soil water content ($\text{cm}^3 \text{ cm}^{-3}$); θ_s and θ_r are the saturated and residual soil water
 149 content ($\text{cm}^3 \text{ cm}^{-3}$), respectively; S is the relative saturation; S_i is the relative saturation at, θ_i , the
 150 initial soil water content ($\text{cm}^3 \text{ cm}^{-3}$); z_s is the length of saturated zone (cm).

151 Correspondingly, the soil hydraulic conductivity in the profile is written as

152
$$K = \begin{cases} K_s & 0 \leq z < z_s & h > -h_d \\ K(h) & z_f \geq z \geq z_s & h_i \leq h \leq -h_d \\ K_i & z \geq z_f & h = h_i \end{cases} \quad (4)$$

153 where K_s is the saturated soil hydraulic conductivity (cm min^{-1}).

154 Then, with Equation (4), the second and third terms on the right side of Equation (1) can
 155 be transformed to

156
$$\int_0^{h_i} K dh = \int_{-h_d}^{h_i} K dh + \int_0^{-h_d} K dh = \int_{-h_d}^{h_i} K dh - K_s h_d \quad (5)$$

157
$$\int_{h_p}^0 K dh = -K_s h_p \quad (6)$$

158 According to Philip (1973), the relationship between F and soil water content can be
 159 described with a simple function:

160
$$F(\theta) = \frac{J_w - K_i}{J_{w0} - K_i} = \frac{\theta - \theta_i}{\theta_s - \theta_i} \quad (7)$$

161 where J_w is the soil water flux (cm min^{-1}). More accurate functions can be found in [Ma et al.](#)
 162 [\(2017a\)](#). No matter what the specific function of F is, F should be 1 in the saturated zone and
 163 gradually decreases from 1 to 0 in the unsaturated wetted zone.

164 Defining the equivalent wetting front length of the unsaturated wetted zone ([Figure 1](#)) as z_{ufe}
 165 by using the piston-type assumption of water flow in [Green & Ampt \(1911\)](#), after considering
 166 Equation (3) and Equation (7), we get

$$167 \quad z_{\text{ufe}} = \frac{\int_{z_s}^{z_f} (\theta - \theta_i) dz}{\theta_s - \theta_i} = (z_f - z_s) B_0 \quad (8)$$

168 where

$$169 \quad B_0 = \int_0^1 \frac{\theta - \theta_i}{\theta_s - \theta_i} d \frac{z - z_s}{z_f - z_s} \quad (9)$$

170 Combining Equation with Equation (8) yields

$$171 \quad \int_0^{z_f} F dz = z_s + \int_{z_s}^{z_f} F dz = z_s + z_{\text{ufe}} \quad (10)$$

$$172 \quad \int_0^{z_f} (K - (1 - F) K_i) dz = K_s z_s + \frac{z_{\text{ufe}}}{B_0} \int_0^1 (K - (1 - F) K_i) d \frac{z - z_s}{z_f - z_s} \quad (11)$$

173 Substituting Equation (5), Equation (6), Equation (10) and Equation (11) in Equation (2)
 174 and rearranging the equation, the expression of J_{w0} related to the length of saturated zone and the
 175 equivalent one of unsaturated wetted zone can be expressed as

$$176 \quad J_{w0} = K_s \left(1 + \frac{B_1 + B_3 - B_2 z_{\text{ufe}}}{z_s + z_{\text{ufe}}} \right) \quad (12)$$

177 where

178
$$B_1 = -\int_{-h_d}^{h_i} \frac{K}{K_s} dh \quad (13)$$

179
$$B_2 = 1 - \frac{\int_0^1 \left(\frac{K}{K_s} - (1-F) \frac{K_i}{K_s} \right) d \frac{z-z_s}{z_f-z_s}}{\int_0^1 F d \frac{z-z_s}{z_f-z_s}} \quad (14)$$

180
$$B_3 = h_p + h_d \quad (15)$$

181 Actually, the expression of J_{w0} can be also derived by applying Darcy's law to the saturated
 182 zone. Soil water flux is evenly distributed with saturated hydraulic conductivity in the saturated
 183 zone. The pressure head should be h_p at the upper boundary of the saturated zone and $-h_d$ at its
 184 bottom.

185 Then,

186
$$J_{w0} = K_s \left(1 + \frac{h_p + h_d}{z_s} \right) = K_s \left(1 + \frac{B_3}{z_s} \right) \quad (16)$$

187 Combining Equation (12) with Equation (16) yields

188
$$z_{ufe} = \frac{B_1 z_s}{B_2 z_s + B_3} \quad (17)$$

189 According to the definition by [Green and Ampt \(1911\)](#), the length of equivalent wetted zone, z_{fe} ,
 190 should be the sum of the saturated zone length, z_s , and the equivalent wetting front length of the
 191 unsaturated zone, z_{ufe} , that is,

192
$$z_{fe} = z_s + z_{ufe} = z_s + \frac{B_1 z_s}{B_2 z_s + B_3} \quad (18)$$

193 Then,

194
$$I = (\theta_s - \theta_i) z_{fc} + K_i t = (\theta_s - \theta_i) \left(z_s + \frac{B_1 z_s}{B_2 z_s + B_3} \right) + K_i t \quad (19)$$

195 where I is the cumulative infiltration or cumulative surface water flux (cm); K_i is normally
 196 negligible in most cases.

197 Since the surface water flux is the derivative of the cumulative infiltration, we obtain other
 198 expression of J_{w0} by neglecting K_i ,

199
$$J_{w0} = \frac{dI}{dt} = (\theta_s - \theta_i) \frac{dz_{fc}}{dt} = (\theta_s - \theta_i) \left(1 + \frac{B_1 B_3}{(B_2 z_s + B_3)^2} \right) \frac{dz_s}{dt} \quad (20)$$

200 Combining Equation (16) and Equation (20) to eliminate J_{w0} and conducting definite
 201 integration of z_s from 0 to z_s and t from 0 to t , we derive the implicit expression of the saturated
 202 zone length with time,

203
$$z_s - (B_3 + B_5) \ln \left(1 + \frac{z_s}{B_3} \right) + B_5 \ln \left(1 + \frac{B_2 z_s}{B_3} \right) + \frac{B_1}{(1 - B_2) B_2} \left(1 - \frac{B_3}{(B_2 z_s + B_3)} \right) = B_4 t \quad (21)$$

204 where

205
$$B_4 = \frac{K_s}{\theta_s - \theta_i} \quad (22)$$

206
$$B_5 = \frac{B_1}{(1 - B_2)^2} \quad (23)$$

207 With Equation (8) and Equation (17), z_f can be derived from z_s

208
$$z_f = z_s + \frac{1}{B_0} z_{ufe} = z_s + \frac{B_1 z_s}{B_0 (B_2 z_s + B_3)} \quad (24)$$

209 Given flux–saturation relationship F , specific soil moisture profile function ($S \sim z$), soil
 210 hydraulic properties ($K \sim h$ and $h \sim \theta$), initial condition (θ_i) and boundary condition (h_p), the length
 211 of saturated zone can be calculated by solving Equation (21). Then, the cumulative infiltration
 212 can be calculated from z_s by using Equation (19). Accordingly, the surface water flux and the
 213 length of the wetted zone can be calculated using Equation (16) and Equation (24), respectively.
 214 Finally, Equation (16), Equation (19), Equation (21) and Equation (24) constitute a new solution
 215 to one-dimensional vertical infiltration with the upper boundary of a constant pressure head. In
 216 order to differentiate the new solution from TGAM and GAME, the new solution is named as
 217 Green-Ampt Model Solution, the GAMS.

218 2.2 A special solution for infiltration with Brooks-Corey model

219 Soil water retention curves and unsaturated hydraulic conductivities can be described using
 220 the model proposed by Brooks and Corey (1964), denoted as the BC model:

221
$$S(h) = \begin{cases} \frac{\theta - \theta_r}{\theta_s - \theta_r} = \left| \frac{h_d}{h} \right|^n & h < -h_d \\ 1 & h \geq -h_d \end{cases} \quad (25)$$

222
$$K(h) = \begin{cases} K_s \left| \frac{h_d}{h} \right|^m = K_s S^{m/n} & h < -h_d \\ K_s & h \geq -h_d \end{cases} \quad (26)$$

223 where $m = (l + 1)n + 2$ with Burdine’s method (Burdine, 1953); l is the soil pore tortuosity factor
 224 and normally $l = 2$ in the BC model.

225 With the upper boundary condition of saturation (i.e. $h = -h_d$), Ma et al. (2015) derived an
 226 expression of soil moisture profile for infiltration into soils with initially uniform soil water
 227 content. Similar expression can be obtained with exactly the same deriving steps in Ma et al.

228 (2015) for the soil water content profile of the unsaturated wetted zone in the current study.
 229 Substituting the length of unsaturated zone here for the length of wetted zone in Ma et al. (2015)
 230 yields,

$$231 \quad S = \left(1 - b \frac{z - z_s}{z_f - z_s} \right)^a \quad (27)$$

232 where

$$233 \quad a = \frac{n}{2n+2} \quad (28)$$

$$234 \quad b = 1 - S_i^{1/a} \quad (29)$$

235 Substituting Equation (25)-(27) to Equation (13) and Equation (14), we get

$$236 \quad B_0 = (\theta_s - \theta_r) \frac{1 - (1 + ab) S_i}{b(a + 1)} \quad (30)$$

$$237 \quad B_1 = \frac{1 - S_i^{3+1/n}}{3n+1} \quad (31)$$

$$238 \quad B_2 = 1 - \frac{(a + 1)(1 - S_i) - (a(a + 2)b - (1 - b)(1 - S_i)) S_i^{3+2/n}}{(1 - (1 + ab) S_i)(a + 2)} \quad (32)$$

239 The other parameter B_3 , B_4 and B_5 can be calculated by Equation (15), Equation (22) and
 240 Equation (23), respectively. Finally, Equation (16), Equation (19), Equation (21) and Equation
 241 (24) constitute a special solution with the BC model compared to the general solution above. The
 242 GAMS in the next part refers to this special solution.

243 3 Materials and methods

244 3.1 Model validation and evaluation

245 As an example, a loam soil with BC model parameters ($\theta_s = 0.434 \text{ cm cm}^{-3}$, $\theta_r = 0.027 \text{ cm}$
246 cm^{-3} , $n = 0.22$, $h_d = 11.15 \text{ cm}$, $K_s = 0.022 \text{ cm min}^{-1}$) was used to validate the performance of the
247 GAMS model. Additionally, the relations with the TGAM and GAME models were investigated
248 regarding their different ways of treating the saturated zone. In order to avoid the disturbance of
249 uncertain errors in real experiments on the theoretical evaluation, the numerical solution of
250 HYDRUS-1D ([Šimůnek et al., 2005](#)) was used as the exact solution to produce the infiltration
251 data needed to validate the new solution. The simulations were also conducted by both analytical
252 and numerical methods to evaluate the influence of the developing saturated zone on infiltration.

253 The GAMS calculation was made following the procedures provided in section 2.2. The
254 calculation of TGAM and GAME followed the same procedures described in [Ma et al. \(2015\)](#).
255 The numerical simulations of the Richards equation were conducted by the HYDRUS-1D
256 software package (version 3.0) for the constant-head 1D vertical infiltration problem ([Šimůnek et](#)
257 [al., 2005](#)). The soil column in the simulation was 200 cm in length with a discrete interval of
258 0.25 cm, and a uniform initial soil moisture distribution ($\theta_i = 0.04 \text{ cm cm}^{-3}$). The upper boundary
259 of a constant water head ($h_p = 0$) and free drainage lower boundary were defined for the
260 simulation. The infiltration time was 2800 min. The soil column was considered as semi-infinite,
261 since the simulation was set to stop before the wetting front reaches the bottom. The simulated
262 surface water flux, cumulative surface water flux, soil water flux and soil water content profiles
263 at time steps of 10 min, 30 min, 60 min, 100 min, 500 min, 1000 min, 1500 min and 2000 min,
264 were directly extracted from the simulated data by HYDRUS-1D. The lengths of the saturated
265 zone (z_s) and wetted zone (z_f) were determined by checking the soil moisture profiles.

266 Specifically, on a soil moisture profile, the depth where soil water content began to be lower than
 267 θ_s was taken as z_s , and the depth where soil water content drop to θ_i was taken as z_f .

268 Relative error (RE) was employed to evaluate the deviation of the three models (GAMS,
 269 GAME and TGAM) from the numerical solution.

$$270 \quad RE_i = \frac{Y_i - O_i}{O_i} \times 100\% \quad (33)$$

271 where Y_i is the simulated value by analytical solutions (GAMS, GAME and TGAM); O_i is the
 272 observed value produced by HYDRUS-1D.

273 3.2 Estimation of model parameters

274 The new GAMS was numerically inverted to obtain the three parameters of soil hydraulic
 275 properties (n , h_d and K_s) from infiltration data (i.e. cumulative infiltration and wetted zone length
 276 versus time). Notably, the method based on the GAMS considered not only the unsaturated zone,
 277 which was ignored in the TGAM based methods (Ma et al., 2017), but also the developing
 278 saturated zone, which was neglected in the GAME method in the first stage of infiltration (Ma et
 279 al., 2017). The estimated soil hydraulic parameters by the methods based on GAMS, GAME and
 280 TGAM were compared to check the influence of the developing saturated zone on the estimation
 281 of soil hydraulic properties.

282 Furthermore, the time-dependent accuracy of analytical solution was investigated. The same
 283 loam soil ($\theta_s = 0.434 \text{ cm cm}^{-3}$, $\theta_r = 0.027 \text{ cm cm}^{-3}$, $\theta_i = 0.04 \text{ cm cm}^{-3}$, $n = 0.22$, $h_d = 11.15 \text{ cm}$, K_s
 284 $= 0.022 \text{ cm min}^{-1}$) was used as the tested soil. The observed time-lapse data (OBS) of cumulative
 285 infiltration and the length of wetted zone were produced by Hydrus-1D for the estimation of soil
 286 hydraulic parameters. Given the known parameters ($\theta_s = 0.434 \text{ cm cm}^{-3}$, $\theta_r = 0.027 \text{ cm cm}^{-3}$, $\theta_i =$

287 0.04 cm cm^{-3}) and the unknown parameters (n , h_d and K_s), the Levenberg-Marquardt algorithm
 288 was employed to minimize the objective function to estimate the unknown parameters (n , h_d and
 289 K_s)

$$290 \quad Q = \sum_{i=1}^N \left(\hat{I}_i(n, h_d, K_s) - I_i \right)^2 + \sum_{i=1}^N \left(\hat{z}_{f,i}(n, h_d, K_s) - z_{f,i} \right)^2 \quad (34)$$

291 where Q is the objective function; \hat{I}_i and I_i are the simulated cumulative infiltration by the GAMS
 292 and the observed data produced by HYDRUS-1D, respectively; $z_{f,i}$ and $\hat{z}_{f,i}$ are the length of
 293 wetted zone simulated by the GAMS and the observed data produced by HYDRUS-1D,
 294 respectively. Details of the methods based on the GAME and TGAM for estimating soil
 295 hydraulic parameters from one-dimensional vertical infiltration can be found in [Ma et al. \(2017\)](#).

296 Moreover, the ratio of the saturated zone length to the effective wetted zone length (denoted
 297 as $LR_{S/EW} = z_s/z_{fe}$ hereafter) in the GAMS was calculated based on Equation (18) and Equation
 298 (21), and its sensitivities to soil texture (listed in [Table 1](#)), initial condition (θ_i) and boundary
 299 condition (h_p) were investigated to theoretically analyze their influences on the development of
 300 the saturated zone. The initial and boundary conditions were defined based on the loam soil ($\theta_s =$
 301 0.434 cm cm^{-3} , $\theta_r = 0.027 \text{ cm cm}^{-3}$, $n = 0.22$, $h_d = 11.15 \text{ cm}$, $K_s = 0.022 \text{ cm min}^{-1}$) with six values
 302 of θ_i (i.e. 0.04 cm cm^{-3} , 0.08 cm cm^{-3} , 0.12 cm cm^{-3} , 0.16 cm cm^{-3} , 0.2 cm cm^{-3} and 0.25 cm cm^{-3})
 303 for $h_p = 0$, and with six values of h_p (i.e. 0 cm , 2 cm , 5 cm , 10 cm , 15 cm and 20 cm) for $\theta_i =$
 304 0.04 cm cm^{-3} .

305

306 **Table 1.** Soil hydraulic properties of different textured soils (Hydrus-1D) and initial conditions
 307 for numerical simulations.

Soil texture	θ_i cm cm ⁻³	θ_r cm cm ⁻³	θ_s cm cm ⁻³	n	h_d cm	K_s cm min ⁻¹
Loamy Sand	0.05	0.035	0.401	0.474	8.70	0.1018
Sandy Loam	0.05	0.041	0.412	0.322	14.66	0.0432
Loam	0.04	0.027	0.434	0.220	11.15	0.0220
Silt	0.03	0.015	0.486	0.211	20.75	0.0113
Sandy Clay Loam	0.08	0.068	0.330	0.250	28.09	0.0072
Clay Loam	0.09	0.075	0.390	0.194	25.91	0.0038
Silty Clay Loam	0.08	0.040	0.432	0.151	32.57	0.0025
Sandy Clay	0.12	0.109	0.321	0.168	29.15	0.0020
Silty Clay	0.10	0.056	0.423	0.127	34.25	0.0015
Clay	0.12	0.090	0.385	0.131	37.31	0.0010

308

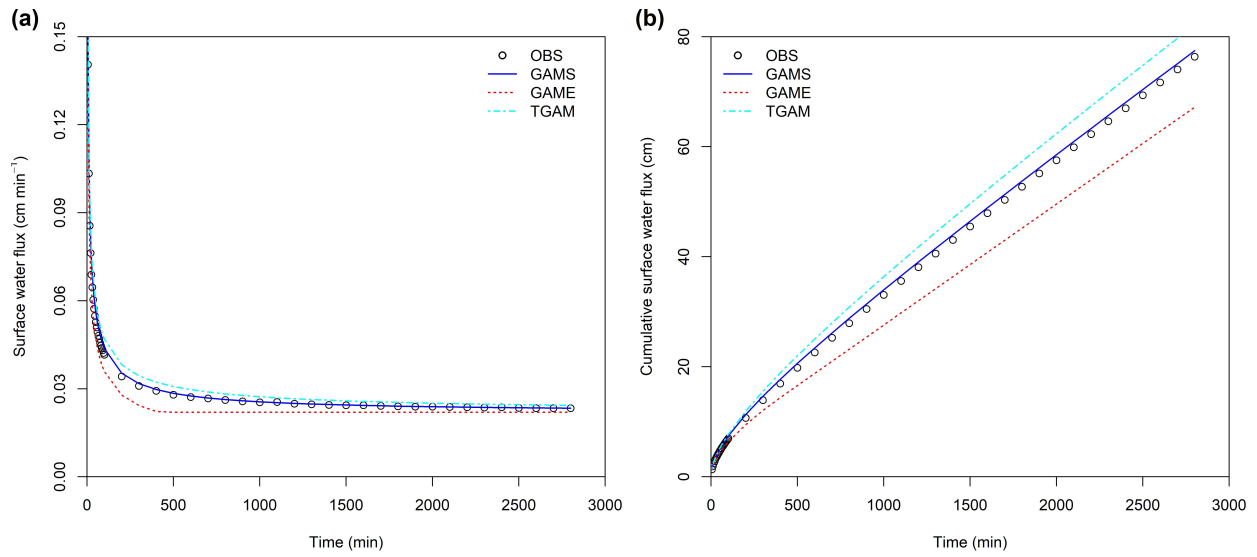
309 **4 Results**

310 4.1 The forward solution for infiltration simulation

311 As depicted in [Figure 2](#) and [Figure 3a](#), the surface water flux, cumulative surface water flux
 312 and wetted zone length simulated by the GAMS with the parameters independently obtained
 313 from soil hydraulic properties agree well with those simulated by HYDRUS-1D for the tested
 314 loam soil. The relative errors of the simulated surface water flux, cumulative surface water flux
 315 and wetted zone length are less than 8% for all time steps and less than 5% for most of the time
 316 steps ([Figure 4](#)). The relative errors of these three infiltration variables are the highest at the
 317 primary stage of the infiltration and gradually drops with the lapsed time. The simulated surface
 318 water flux is very close to the exact solution with relative errors close to 0 after 500 min ([Figure](#)
 319 [4a](#)). The relative errors of the simulated cumulative surface water flux and wetted zone length
 320 decrease to about 2% after 500 min ([Figure 4b and 4c](#)). As shown in [Figure 3b](#), the GAMS give
 321 accurate estimates of the saturated zone length all along the time. However, the GAMS seems to

322 slightly overestimate the length of the unsaturated zone but with no increasing deviation (Figure
323 3c). This should be responsible for the 2% relative errors of the simulated cumulative surface
324 water flux and wetted zone length in the later stage of the infiltration. Generally, the soil
325 moisture profiles simulated by the GAMS agree well with the those simulated by HYDRUS-1D
326 from a long time perspective but slight deviation exists in the initial short time of infiltration
327 (Figure 5).

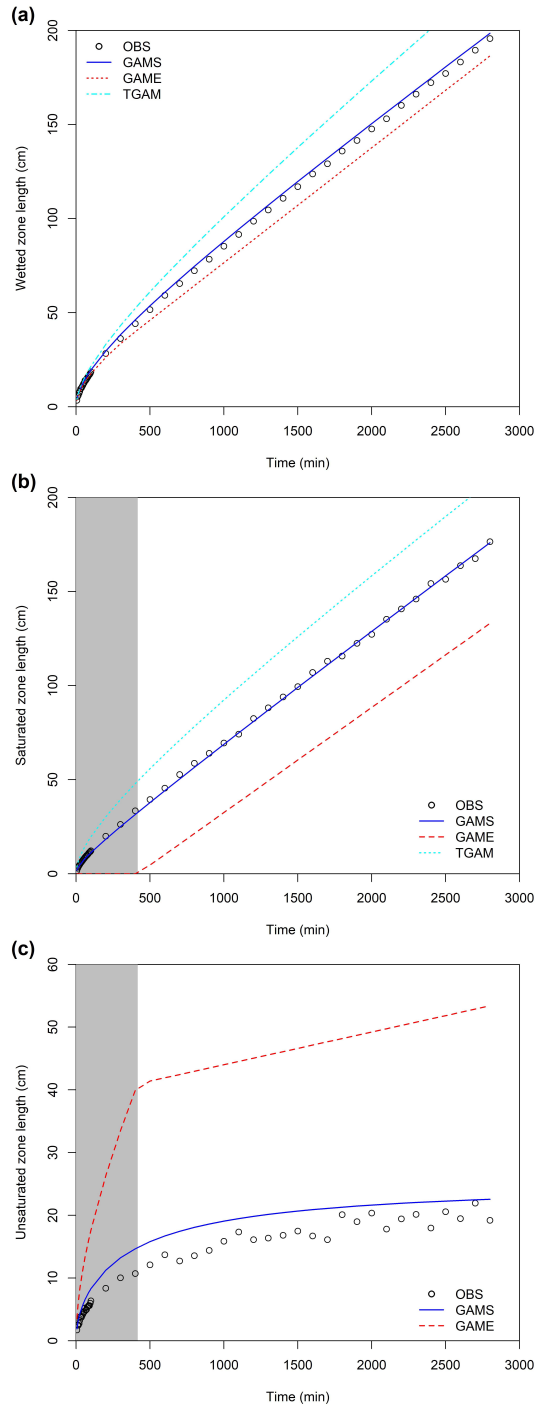
328 In general, the novel GAMS model enables a more accurate simulation of infiltration
329 process than the GAME and TGAM models for a loam soil (Figures 2-5). Obviously, the TGAM
330 overestimated the surface water flux, cumulative surface water flux, and the length of the wetted
331 zone with REs of about 10%-18%. The GAME underestimated the surface water flux,
332 cumulative surface water flux and the length of wetted zone with REs of about 10%. The GAMS
333 gave the best simulations with the smallest and decreasing REs among the three models. Only in
334 the first stage of infiltration, the simulation accuracy of the GAME (Figure 4) is comparable to
335 and even higher than the GAMS (Figure 4c, Figure 5). However, in the first stage of infiltration,
336 the GAME shows increasing errors (Figure 3c, Figure 4). In the second stage of infiltration, the
337 surface water flux was still underestimated by the GAME with REs of about -10%. It should be
338 noted that the GAME simulated the soil moisture profiles better than the GAMS in the first stage
339 but the REs of the GAME substantially increased after the critical time (Figure 5).



340

341 **Figure 2.** Simulated (a) surface water flux, and (b) cumulative surface water flux by the GAMS,
 342 GAME and TGAM, respectively, compared with the observed data (OBS) produced by the
 343 numerical solution (HYDRUS-1D) for a loam soil.

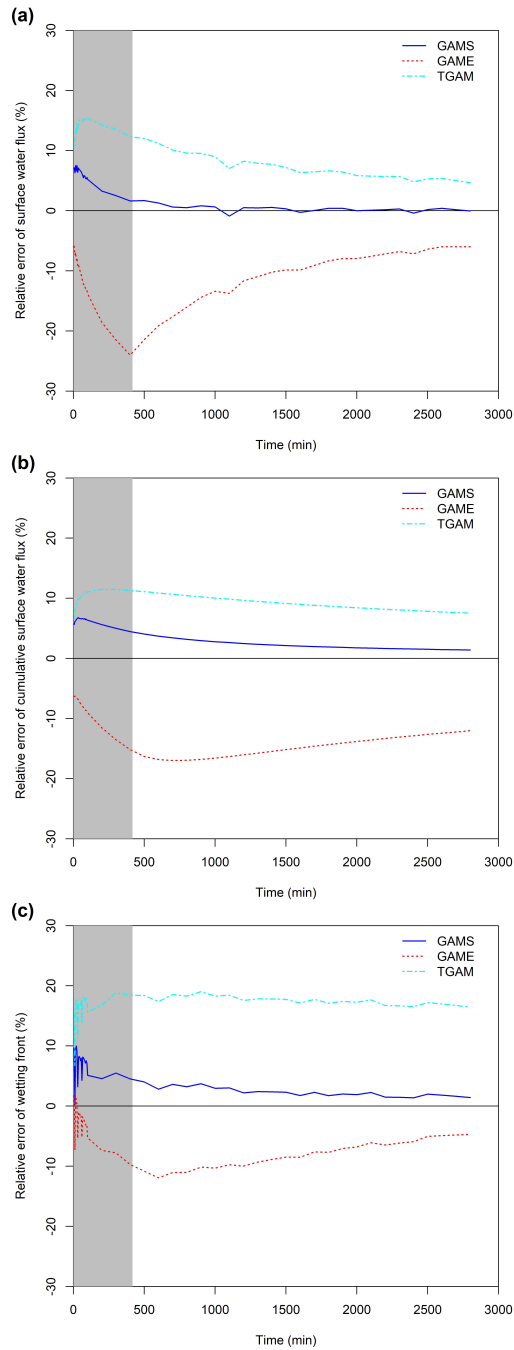
344



345

346 **Figure 3.** Simulated lengths of (a) wetted zone, (b) saturated zone, and (c) unsaturated zone by
 347 the GAMS, GAME and TGAM, respectively, compared with the observed data (OBS) produced
 348 by the numerical solution (HYDRUS-1D) for a loam soil.

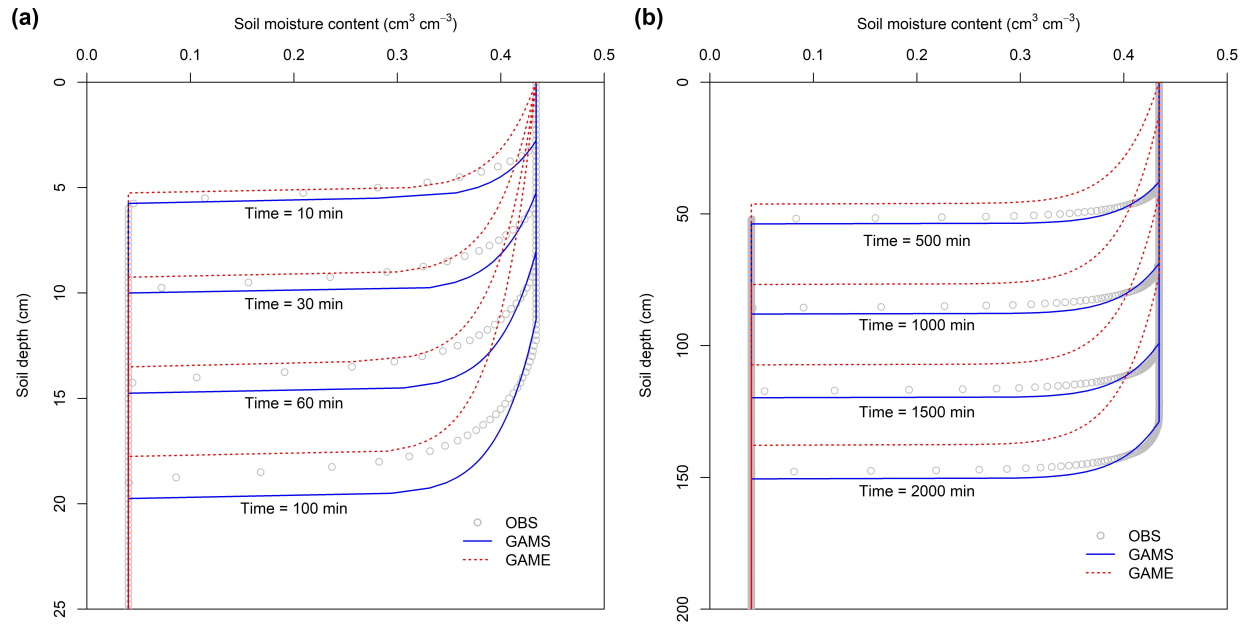
349



350

351 **Figure 4.** Relative error (RE) of (a) surface water flux, (b) cumulative surface water flux and (c)
 352 length of wetted zone simulated by the GAMS, GAME and TGAM, respectively, to that by the
 353 numerical solution (HYDRUS-1D) for a loam soil. The gray zone represents the infiltration
 354 before the critical time calculated by equation (29) in Ma et al. (2015).

355



356

357 **Figure 5.** Simulated soil moisture profiles in (a) short infiltration time and (b) long infiltration
 358 time by the GAMS and GAME, respectively, compared with the observed data (OBS) produced
 359 by the numerical solution (HYDRUS-1D) for a loam soil.

360

4.2 The influence of saturated zone on the estimation of soil hydraulic properties

361

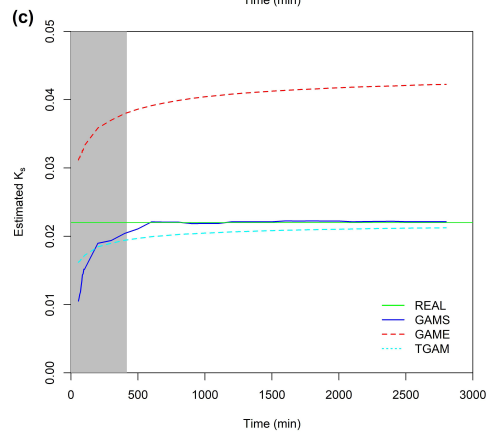
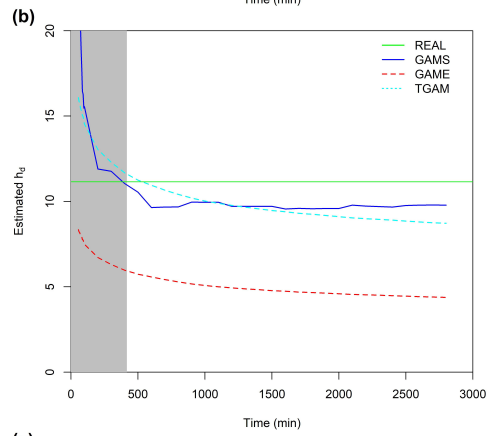
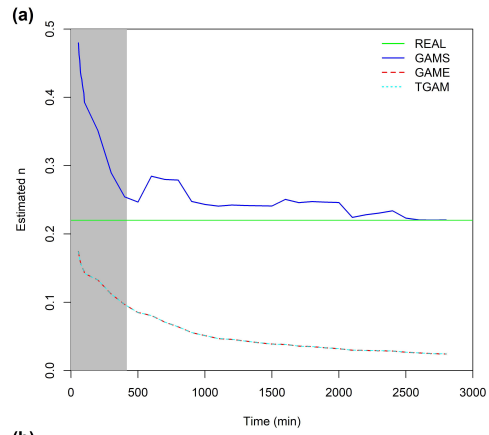
362 **Figure 6** shows the estimated parameters of soil hydraulic properties for a loam soil by
 363 inverting the GAMS, GAME and TGAM models. The estimated values of n and h_d by these
 364 three models exhibit a similar decline tendency along the infiltration time, while the estimated
 365 values of K_s increase with the infiltration time. Generally, the estimated parameters by the
 366 GAMS are closer to the real values compared with those by the GAME. The values of n
 367 estimated by the TGAM is equal to those by the GAME, while the estimated values of h_d and K_s
 368 by the TGAM are close to those by the GAMS. The results indicate that the critical time is
 369 important for the estimation accuracy of the hydraulic parameters. Before the critical time,
 370 especially in a short time, the estimated parameters by the GAME show relatively lower errors
 than that by the GAMS. After the critical time, however, the estimation by the GAMS exhibits a

371 higher accuracy than that by the GAME. Whether in a short or long time, the inverting of the
372 TGAM cannot simultaneously give accurate estimates of n , h_d and K_s . Generally, the GAMS
373 improved the estimate accuracy of soil hydraulic properties by the infiltration models from the
374 infiltration process after the critical time.

375 4.3 The sensitivity analysis of saturated zone length

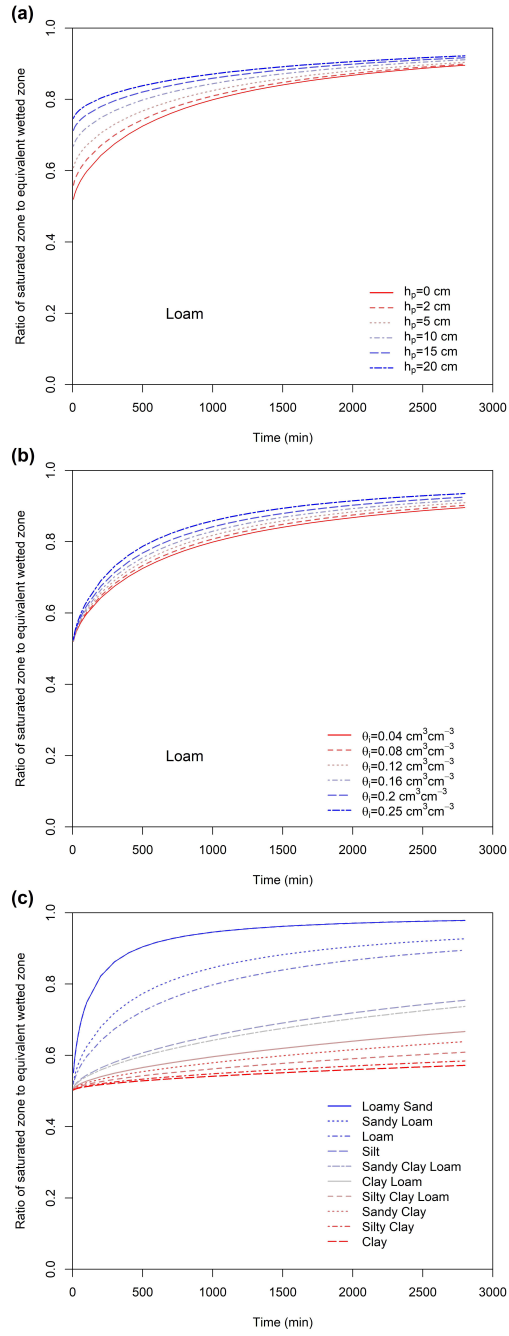
376 As shown in Figure 7, $LR_{S/EW}$ can be affected by soil properties (i.e. soil texture), boundary
377 conditions (i.e. surface water depth), and initial conditions (i.e. initial soil water content).
378 Without ponding water over soil surface, the values of $LR_{S/EW}$ were initially equal to 0.5,
379 increased with infiltration time and approached to 1 at infinity. Increased ponding depth can
380 promote the proportion of the saturated zone especially at the initial stage of infiltration but its
381 effects attenuate with time (Figure 7a). The $LR_{S/EW}$ increased with elevating initial soil water
382 content while little influence can be found at the initial stage of infiltration (Figure 7b).
383 Obviously, soil texture shows the greatest effect on the development of saturated zone (Figure
384 7c). The $LR_{S/EW}$ for a clay soil increased slowly with time and was close to 0.5 for most of time.
385 The results indicate that the coarser the soil texture, the greater the $LR_{S/EW}$ at the same infiltration
386 time. The $LR_{S/EW}$ for a loamy sandy soil increased rapidly and approached to 1 as infiltration
387 continued.

388 As shown in Figure 8a, $LR_{S/EW}$ can also be affected by soil hydraulic properties, that is, the
389 shape coefficient n of soil water retention curve, water-entry suction h_d , and saturated hydraulic
390 conductivity K_s . A higher n value caused a lower fraction of saturated zone (Figure 8a) during
391 infiltration. A greater value of h_d resulted in a lower $LR_{S/EW}$ (Figure 8b). A higher value of K_s
392 accelerated the development of z_s (Figure 8c). Compared to h_d and K_s , the influence of the shape
393 coefficient n on $LR_{S/EW}$ seems to be negligible.



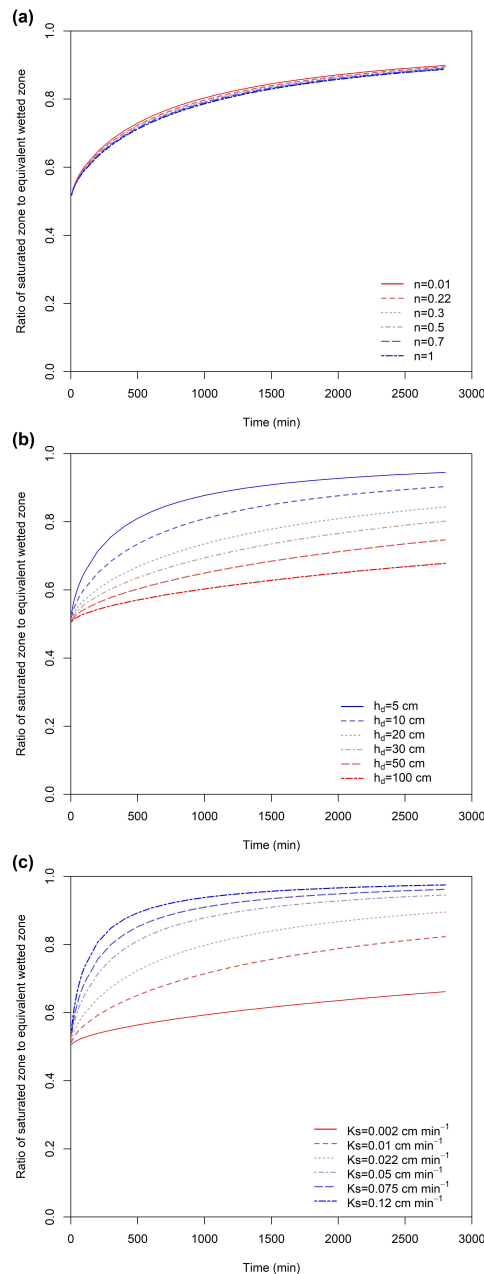
396 **Figure 6.** Time-dependent (a) shape coefficient n , (b) water-entry suction h_d , and (c) saturated
397 hydraulic conductivity K_s estimated by model inversion of GAMS, GAME and TGAM,
398 respectively, with the observed data of different infiltration time, compared with the real
399 parameter values (REAL) of a loam soil. The gray zone represents the infiltration before the
400 critical time calculated by equation (29) in Ma et al. (2015).

401



403 **Figure 7.** Sensitive analysis of the length ratio of saturated zone to equivalent wetted zone
 404 $LR_{S/EW}$ to (a) surface water depth ($h_p = 0$ cm, 2 cm, 5 cm, 10 cm, 15 cm and 20 cm) for a loam
 405 soil, (b) initial soil water content ($\theta_i = 0.04$ cm cm⁻³, 0.08 cm cm⁻³, 0.12 cm cm⁻³, 0.16 cm cm⁻³,
 406 0.2 cm cm⁻³ and 0.25 cm cm⁻³) for a loam soil, and (c) soil texture (see in Table 1) by using the
 407 GAMS.

408



409

410 **Figure 8.** Sensitive analysis of the length ratio of saturated zone to equivalent wetted zone
 411 $LR_{S/EW}$ to (a) the shape coefficient n ($n = 0.01, 0.22, 0.3, 0.5, 0.7$ and 1), (b) water-entry suction
 412 h_d ($h_d = 5$ cm, 10 cm, 20 cm, 30 cm, 50 cm and 100 cm), and (c) saturated hydraulic conductivity
 413 K_s ($K_s = 0.002$ cm min⁻¹, 0.01 cm min⁻¹, 0.022 cm min⁻¹, 0.05 cm min⁻¹, 0.075 cm min⁻¹ and 0.12
 414 cm min⁻¹) for a loam soil by using the GAMS.

415

416 **5 Discussion**

417 5.1 The factors influencing the development of saturated zone

418 The results in [Figure 7a](#) agree well with the early research by [Philip \(1958b\)](#). A higher
 419 ponding depth on the surface can promote the development of saturated zone, which can be
 420 deduced by Equation (12) and Equation (15). Initially wetter soils have smaller space for further
 421 water storage and narrower range of soil moisture in the wetted zone. Thus, the saturated zone
 422 developed more quickly in a wet soil than in a dry soil ([Philip, 1958a](#)), which was confirmed by
 423 the results in [Figure 7b](#).

424 Soil texture could affect the development of saturated zone mainly from three aspects: (a)
 425 the shape coefficient n , which reflects soil pore size distribution; (b) water-entry suction h_d ,
 426 which is related to the maximum equivalent capillary pore size of a soil, and (c) saturated
 427 hydraulic conductivity K_s . A higher n value represents a steeper pore size distribution which is
 428 closer to the delta-type soil water diffusivity and could cause a lower fraction of saturated zone
 429 during infiltration as shown in [Figure 8a](#). Since soil is tension-saturated when $0 > h > -h_d$ ([Philip,](#)
 430 [1958a](#)), the water-entry suction shall have contrary impacts on the saturated zone to h_p from
 431 Equation (12) and Equation (15). A greater value of h_d resulted in a lower $LR_{S/EW}$. The parameter

432 B_4 is the average velocity of pore water under gravity gradient which corresponds to the cases in
 433 a large infiltration time. For a given soil porosity, B_4 is positively correlated to K_s . According to
 434 Equation (21), a higher value of K_s will accelerate the development of z_s as shown in [Figure 8c](#).
 435 In contrast to a fine-textured soil, a coarse-textured soil normally has greater K_s and n but lower
 436 h_d . Obviously, the positive effects of K_s and h_d on $LR_{S/EW}$ overwhelmed the negative effect of n ,
 437 which can explain the results shown in [Figure 7c](#).

438 5.2 The influence of saturated zone on infiltration

439 The key character differentiating the GAMS from the TGAM and GAME models is its
 440 consideration of the wetting zone composed of both saturated and unsaturated zones. The TGAM
 441 was derived by assuming a piston-type soil moisture profile, that is, a fully saturated wetting
 442 zone ([Green & Ampt, 1911](#)). While, in the GAME, the wetting zone was considered unsaturated
 443 before a critical time, when the surface water flux dropped to K_s , and after which the saturated
 444 zone developed linearly with time ([Ma et al., 2015](#)). Insight into the internal relationships of the
 445 GAMS with the TGAM and GAME could provide an improved understanding on the influence
 446 of the saturated zone on infiltration.

447 With the definition of Equation (18), the Equation (12) can be rewritten as

$$448 J_{w0} = K_s \left(1 + \frac{B_1 + B_3}{z_{fe}} \right) - K_s B_2 \left(1 - \frac{z_s}{z_{fe}} \right) \quad (35)$$

449 The first term on the right side of Equation (35) is equal to the TGAM which is characterized by
 450 piston-type water profile and average pressure head at the wetting front (i.e. Equation (13)) with
 451 the form of [Neuman \(1976\)](#). The second term on the right side of Equation (35) represents the
 452 influence of the saturated zone on surface soil water flux. For a soil with delta-type water

453 diffusivity, a piston-type water profile is expected and z_s is close to z_{fe} . Then, the GAMS
 454 (Equation (35)) can be transformed to the TGAM, given:

$$455 \quad J_{w0} = K_s \left(1 + \frac{B_1 + B_3}{z_{fe}} \right) \quad (36)$$

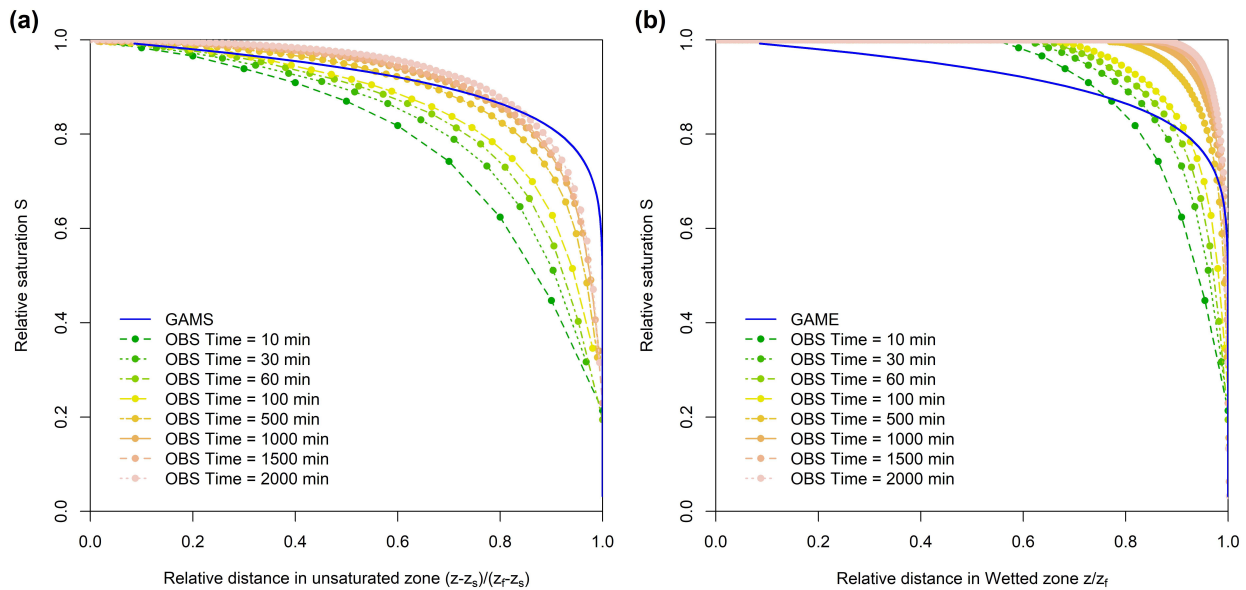
456 For a soil with water diffusivity far from delta-type, a non-piston-type water profile and a
 457 low length ratio of the saturated zone to wetted zone are expected. If neglecting the development
 458 of saturated zone (i.e. $z_s = 0$), the GAMS (Equation (35)) can be transformed to the GAME, that
 459 is,

$$460 \quad J_{w0} = K_s \left(1 + \frac{B_1 + B_3}{z_{fe}} \right) - K_s B_2 = (1 - B_2) K_s \left(1 + \frac{B_1 + B_3}{(1 - B_2) z_{fe}} \right) \quad (37)$$

461
 462 As depicted in Equation (35), it is $LR_{S/EW}$ rather than the saturated zone length that leads the
 463 transformations of the GAMS model to GAME and TGAM models. Obviously, the TGAM
 464 overestimated the surface water flux and thus cumulative surface water flux, and the length of
 465 the wetted zone because the wetting zone was considered overall saturated as shown in Equation
 466 (36). Neglecting the development of the saturated zone as shown in Equation (37) resulted in the
 467 underestimation of the surface water flux by the GAME. In contrast, a developing saturated zone
 468 was accurately characterized in the GAMS as shown in Equation (35), which contributed to the
 469 best simulations among the three models.

470 However, in the first stage of infiltration, $LR_{S/EW}$ was relatively small (Figure 7) and same
 471 to the effects of saturated zone on the surface water flux. In addition, the soil moisture profile
 472 shape in GAME was closer to the real one in the first stage than that in the GAMS (Figure 9),

473 which will be discussed in details in the section 5.3. Consequently, the simulation or estimation
 474 accuracy of the GAME (Figure 4) is comparable to and even higher than the GAMS (Figure 4c,
 475 Figure 5) in the first stage of infiltration. Nevertheless, $LR_{S/EW}$ and the effects of saturated zone
 476 on the surface water flux increased with time (Figure 7). Then, the simulation errors of the
 477 GAME rose up (Figure 3c, Figure 4) as the saturated zone was completely ignored (Figure 3b).
 478 Although a linearly increasing saturated zone length was considered in the second stage of
 479 infiltration (Figure 3b), it is not enough to fully characterize the developing saturated zone and
 480 thus the surface water flux was still underestimated.



481
 482 **Figure 9.** Comparison of the simulated relative soil moisture profile by (a) the GAMS, and (b)
 483 the GAME to the observed data (OBS) produced by the numerical solution (HYDRUS-1D) for a
 484 loam soil.

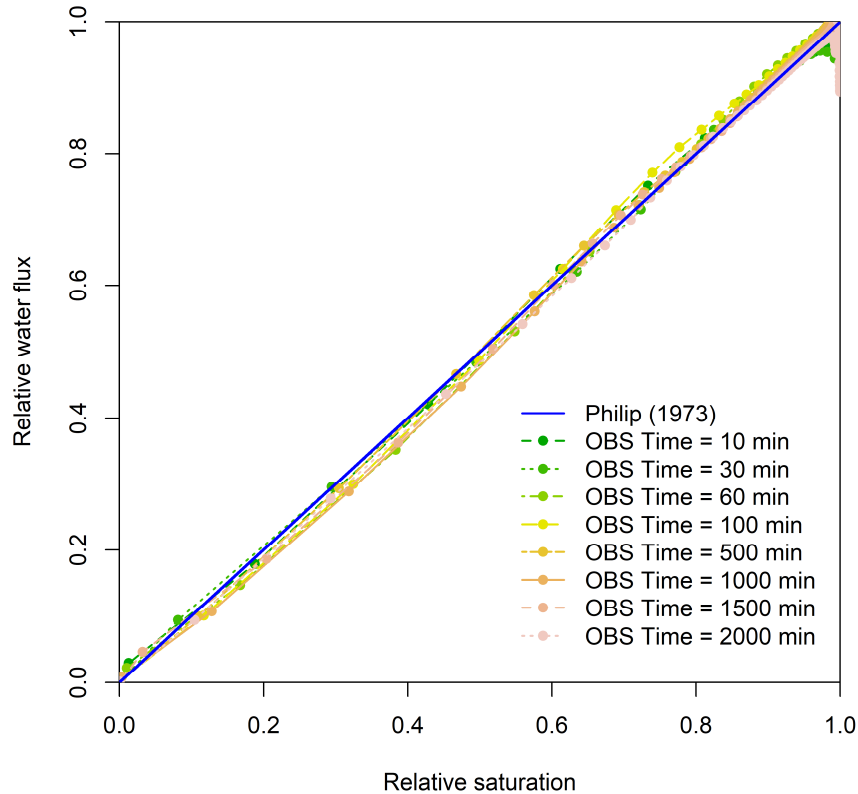
5.3 The factors causing the deviation of the GAMS

486 That the GAMS exhibits relatively larger errors in the simulated water fluxes in short
 487 infiltration times than those in long infiltration times could be induced by the two assumptions of

488 time-independency in soil water flux-saturation relationship (Equation (7)) and relative soil
489 moisture profile (Equation (3)) in the unsaturated zone for the derivation of the GAMS.

490 According to the theoretical analysis by Philip (1973), the soil water flux-saturation
491 relationship in the form of Equation (7) represents the case of coarse-textured soils, that are,
492 linear soils or “delta-function” soils. For natural soils, it may vary with soil texture, infiltration
493 time and boundary conditions but will converge to the curve of Equation (7) in the long
494 infiltration time (Philip, 1973). The texture-dependency of soil water flux-saturation relationship
495 has been confirmed by the observed data in White (1979) and Ma et al. (2017). More accurate
496 expressions for the soil water flux-saturation relationship can be found in literatures (Evangelides
497 et al., 2005; Kargas et al., 2019; Ma et al., 2017; Vauclin and Haverkamp, 1985). Actually, the
498 soil water flux-saturation relationship depended little on time especially in a short infiltration
499 period (Ma et al., 2017) and did not exert obvious influences on infiltration simulations
500 (Haverkamp et al., 1990; Hogarth et al., 2011). Moreover, the expression of Equation (7) has
501 been successfully used for deriving accurate approximate analytical solutions of infiltration
502 problems from Richards equation (Assouline, 2013; Haverkamp et al., 1990; Hogarth et al.,
503 2011; Ma et al., 2015). Although more accurate expression than Equation (7) can be adapted to
504 improve the infiltration simulation (Hayek, 2018), the corresponded solutions are more complex
505 for practical application. For the loam soil in this research, no obvious time-dependency can be
506 found in the soil water flux-saturation relationship and the Equation (7) in the GAMS exhibits
507 enough accuracy as shown in Figure 10. It seems impossible that the relatively great errors of the
508 surface water flux simulated by the GAMS (Figure 4) was caused by the assumption of soil
509 water flux-saturation relationship inherent in Equation (7).

510 The assumption of time-dependent soil moisture profile shape simplified the derivation of
511 the GAMS. Actually, the relative soil moisture profile in the unsaturated zone for the loam soil
512 exhibits time-dependency in short infiltration time and approaches to a steady shape only in long
513 infiltration time (Figure 9). Consequently, the deviation of the simulated soil moisture profiles by
514 the GAMS from those by HYDRUS-1D is mainly in the early infiltration stage and exhibits in
515 two aspects (Figure 5): (1) the overestimated length of unsaturated zone, (2) the twisted shape of
516 soil moisture profiles in the unsaturated zone. Including the developing saturated zone makes the
517 simulated relative soil moisture profiles by the GAMS closer to the steady shape in the long
518 infiltration time (Figure 9a) while the GAME yielded a relative soil moisture profile closer to the
519 unsteady shape in the short time for no consideration of saturated zone (Figure 9b). In addition,
520 the expression for calculating the length of unsaturated zone was derived based on the soil
521 moisture profile of Equation (3) in the unsaturated zone. Therefore, it could be concluded that
522 the simulation errors of the GAMS in the short time is mainly induced by the errors in the
523 function of relative soil moisture profile in the unsaturated zone.



524

525 **Figure 10.** Comparison of the simulated soil water flux-saturation relationship by the numerical
 526 solution (HYDRUS-1D) and the expression proposed by Philip (1973) for a loam soil.

527

528 Actually, the expression of the relative soil moisture profile (i.e. Equation (3)) in both the
 529 GAME and GAMS was derived based on Equation (7) and an approximation of time-
 530 independent soil potential profile shape (Equation (A6) in [Ma et al. \(2015\)](#)). A more accurate
 531 description of soil water flux-saturation relationship and the consideration of the time-
 532 dependency of soil moisture profile shape are expected to further improve the accuracy of soil
 533 moisture profile simulation ([Hayek, 2018](#); [Hogarth et al., 2013](#); [Hogarth et al., 2011](#)).
 534 Unfortunately, it is difficult to derive such a time-dependent expression of soil moisture profile
 535 shape in the current study, given the complex relationship between soil moisture profile and soil

536 water flux (Haverkamp et al., 1990; Hogarth et al., 2011). A recent work by Su et al. (2018)
537 proposed an expression of time-dependent soil moisture profile shape. However, it makes the
538 derivation of infiltration model difficult and fails at a large infiltration time.

539 5.4 The general use of the GAMS

540 Based on the assumptions of time-independency of soil water flux-saturation relationship
541 and relative soil moisture profile, the GAMS was derived with no limitation of the specific form
542 of relative soil moisture profile and soil hydraulic properties. According to Wang et al. (2013)
543 and Ma et al. (2015, 2017b), the form of relative soil moisture profile depends on the specific
544 function of soil hydraulic properties and soil water flux-saturation relationship, and the shape
545 coefficient of soil moisture profile is only related with the shape parameter of the soil water
546 retention curve. Given the soil moisture profile function derived for a specific soil hydraulic
547 property model (e.g. BC model, VG model), it is easy to obtain the parameters of the GAMS by
548 Equation (9), Equations (13)-(15) and Equations (22)-(23) from soil hydraulic properties.
549 Furthermore, other forms of soil water flux-saturation relationship (Evangelides et al., 2005; Ma
550 et al., 2017) can be also included in the novel GAMS by substituting the soil water flux-
551 saturation relationship in Philip (1973).

552 In the future, more accurate unsaturated soil moisture profile functions are expected to be
553 adopted in the GAMS to further improve the infiltration simulation and soil hydraulic parameters
554 estimation. Moreover, the general solution of the GAMS should be extended from uniform soils
555 to stratified soils or soils with non-uniform initial soil moisture profile, as well as the soils with
556 more hydraulic property models such as the VG model (van Genuchten, 1980).

557 6 Conclusions

558 Ponding at the soil surface changes surface pressure head and affects soil moisture profile
559 shape in infiltration. A novel analytical solution, the GAMS, is derived to one-dimensional
560 vertical infiltration under ponding conditions for any forms of soil hydraulic properties models,
561 which can describe the length of saturated zone versus infiltration time with a simple expression.
562 The GAMS was evaluated with a special solution for Brooks-Corey soil hydraulic property
563 model. Compared with the TGAM model (Green and Ampt, 1911) and GAME model (Ma et al.,
564 2015), the GAMS showed a better performance in infiltration simulation indicated by higher
565 agreement with the numerical solution by HYDRUS-1D along the infiltration period.
566 Furthermore, the model inversion of the GAMS yields more accurate estimates of soil hydraulic
567 property model parameters from a one-dimensional vertical infiltration experiment. Besides, the
568 time-dependency of model parameter estimation by the GAMS is weaker in long infiltration time
569 than the TGAM and GAME models. The novel GAMS is supposed to be used in irrigation
570 design and rainfall-runoff simulation by providing more accurate data of cumulative infiltration
571 and soil moisture distribution.

572

573

574

575 Acknowledgments

576 This work was supported by the National Natural Science Foundation of China (No.
577 42177292), the Strategic Priority Research Program of the Chinese Academy of Sciences (Grant
578 No. XDA28010401), and the earmarked fund for China Agriculture Research System (CARS-03,
579 CARS-52).

580 Data Availability Statement

581 The data set used to validate the new solution was produced by the HYDRUS-1D software
582 (version 3.0) (Šimůnek et al., 2005). The program to calculate and draw figures is edited in R
583 language (version 4.1.2) (R Core Team, 2021). All the data set and program are available after
584 requested.

585 References

- 586 Angulo-Jaramillo, R., V. Bagarello, S. Di Prima, A. Gosset, M. Iovino, and L. Lassabatere
587 (2019), Beerkan Estimation of Soil Transfer parameters (BEST) across soils and scales,
588 *Journal of Hydrology*, 576, 239-261. doi:10.1016/j.jhydrol.2019.06.007
- 589 Assouline, S. (2013), Infiltration into soils: Conceptual approaches and solutions, *Water*
590 *Resources Research*, 49(4), 1755-1772. doi:10.1002/wrcr.20155
- 591 Assouline, S., J. S. Selker, and J. Y. Parlange (2007), A simple accurate method to predict time of
592 ponding under variable intensity rainfall, *Water Resources Research*, 43(3), W03426.
593 doi:10.1029/2006wr005138
- 594 Bonetti, S., Z. W. Wei, and D. Or (2021), A framework for quantifying hydrologic effects of soil
595 structure across scales, *Commun Earth Environ*, 2(1). doi:10.1038/s43247-021-00180-0
- 596 Brutsaert, W. (1977), Vertical infiltration in dry soil, *Water Resources Research*, 13(2), 363-368.
597 doi:10.1029/WR013i002p00363

- 598 Burdine, N. T. (1953), Relative Permeability Calculations from Pore Size Distribution Data, *T*
599 *Am I Min Met Eng*, 198, 71-78. doi:10.2118/225-G
- 600 Corradini, C., F. Melone, and R. E. Smith (1994), Modeling Infiltration during Complex Rainfall
601 Sequences, *Water Resources Research*, 30(10), 2777-2784. doi:10.1029/94wr00951
- 602 Corradini, C., F. Melone, and R. E. Smith (1997), A unified model for infiltration and
603 redistribution during complex rainfall patterns, *Journal of Hydrology*, 192(1-4), 104-124.
604 doi:10.1016/S0022-1694(96)03110-1
- 605 Evangelides, C., C. Tzimopoulos, and G. Arampatzi (2005), Flux-saturation relationship for
606 unsaturated horizontal flow, *Soil Science*, 170(9), 671-679.
607 doi:10.1097/01.ss.0000185904.72717.4c
- 608 Fatichi, S., D. Or, R. Walko, H. Vereecken, M. H. Young, T. A. Ghezzehei, T. Hengl, S. Kollet,
609 N. Agam, and R. Avissar (2020), Soil structure is an important omission in Earth System
610 Models, *Nat Commun*, 11(1), 522. doi:10.1038/s41467-020-14411-z
- 611 Green, W. H., and G. A. Ampt (1911), Studies on Soil Physics, *The Journal of Agricultural*
612 *Science*, 4(01), 1-24. doi:10.1017/S0021859600001441
- 613 Haverkamp, R., P. J. Ross, K. R. J. Smettem, and J. Y. Parlange (1994), 3-dimensional analysis
614 of infiltration from the disc infiltrometer .2. physically-based infiltration equation, *Water*
615 *Resources Research*, 30(11), 2931-2935. doi:10.1029/94wr01788
- 616 Haverkamp, R., J. Y. Parlange, J. L. Starr, G. Schmitz, and C. Fuentes (1990), Infiltration under
617 Poned Conditions .3. A Predictive Equation Based on Physical Parameters, *Soil Science*,
618 149(5), 292-300. doi:10.1097/00010694-199005000-00006
- 619 Hayek, M. (2018), An efficient analytical model for horizontal infiltration in soils, *Journal of*
620 *Hydrology*, 564, 1120-1132. doi:10.1016/j.jhydrol.2018.07.058

- 621 Hogarth, W. L., D. A. Lockington, D. A. Barry, M. B. Parlange, R. Haverkamp, and J. Y.
622 Parlange (2013), Infiltration in soils with a saturated surface, *Water Resources Research*,
623 49(5), 2683-2688. doi:10.1002/wrcr.20227
- 624 Hogarth, W. L., D. A. Lockington, D. A. Barry, M. B. Parlange, G. C. Sander, L. Li, R.
625 Haverkamp, W. Brutsaert, and J. Y. Parlange (2011), Analysis of time compression
626 approximations, *Water Resources Research*, 47, W09501. doi:10.1029/2010WR010298
- 627 Horton, R. E. (1941), An Approach Toward a Physical Interpretation of Infiltration-Capacity, *Soil*
628 *Science Society of America Journal*, 5(C), 399-417.
629 doi:10.2136/sssaj1941.036159950005000C0075x
- 630 Jaiswal, P., Y. Gao, M. Rahmati, J. Vanderborght, J. Šimůnek, H. Vereecken, and J. A. Vrugt
631 (2022), Parasite inversion for determining the coefficients and time-validity of Philip's two-
632 term infiltration equation, *Vadose Zone J.*, 21(1), e20166. doi:10.1002/vzj2.20166
- 633 Kargas, G., and P. A. Londra (2021), Comparison of Two-Parameter Vertical Poned Infiltration
634 Equations, *Environmental Modeling & Assessment*, 26(2), 179-186. doi:10.1007/s10666-
635 020-09727-5
- 636 Kargas, G., P. Londra, and P. Kerkides (2019), Investigation of the Flux–Concentration Relation
637 for Horizontal Flow in Soils, *Water*, 11(12), 2442. doi:10.3390/w11122442
- 638 Klopp, H. W., and A. L. M. Daigh (2020), Soil hydraulic model parameters and methodology as
639 affected by sodium salt solutions, *Soil Sci Soc Am J*, 84(2), 354-370. doi:10.1002/saj2.20015
- 640 Kostiakov, A. N. (1932), On the Dynamics of the Coefficient of Water Percolation in Soils and
641 on the Necessity for Studying it from a Dynamic Point of View for Purpose of Amelioration,
642 paper presented at Transactions of 6th Committee International Society of Soil Science,
643 Russia.

- 644 Ma, D. H., Q. J. Wang, and M. A. Shao (2009), Analytical Method for Estimating Soil Hydraulic
645 Parameters from Horizontal Absorption, *Soil Science Society of America Journal*, 73(3),
646 727-736. doi:10.2136/sssaj2008.0050
- 647 Ma, D. H., J. B. Zhang, and Y. X. Lu (2017), Derivation and Validation of a New Soil Pore-
648 Structure-Dependent Flux–Saturation Relationship, *Vadose Zone J.*, 16(5).
649 doi:10.2136/vzj2016.11.0117
- 650 Ma, D. H., J. B. Zhang, J. B. Lai, and Q. J. Wang (2016), An improved method for determining
651 Brooks–Corey model parameters from horizontal absorption, *Geoderma*, 263, 122-131.
652 doi:10.1016/j.geoderma.2015.09.007
- 653 Ma, D. H., J. B. Zhang, Y. X. Lu, L. s. Wu, and Q. J. Wang (2015), Derivation of the
654 Relationships between Green–Ampt Model Parameters and Soil Hydraulic Properties, *Soil
655 Science Society of America Journal*, 79(4), 1030-1042. doi:10.2136/sssaj2014.12.0501
- 656 Ma, D. H., J. B. Zhang, R. Horton, Q. J. Wang, and J. B. Lai (2017), Analytical Method to
657 Determine Soil Hydraulic Properties from Vertical Infiltration Experiments, *Soil Science
658 Society of America Journal*, 81(6), 1303-1314. doi:10.2136/sssaj2017.02.0061
- 659 Mezenzev, V. J. (1948), Theory of formation of the surface runoff, *Meteorol I Hidrologia*(3), 33–
660 46
- 661 Morbidelli, R., C. Corradini, C. Saltalippi, A. Flammini, J. Dari, and R. S. Govindaraju (2018),
662 Rainfall Infiltration Modeling: A Review, *Water*, 10(12). doi:10.3390/w10121873
- 663 Moret-Fernández, D., B. Latorre, M. V. López, Y. Pueyo, L. Lassabatere, R. Angulo-Jaramilo, M.
664 Rahmati, J. Tormo, and J. M. Nicolau (2020), Three- and four-term approximate expansions
665 of the Haverkamp formulation to estimate soil hydraulic properties from disc infiltrometer
666 measurements, *Hydrological Processes*, 34(26), 5543-5556. doi:10.1002/hyp.13966

- 667 Neuman, S. P. (1976), Wetting Front Pressure Head in Infiltration-Model of Green and Ampt,
668 *Water Resources Research*, 12(3), 564-566. doi:10.1029/WR012i003p00564
- 669 Parlange, J. Y. (1971), Theory of Water-Movement in Soils .2. One-Dimensional Infiltration, *Soil*
670 *Science*, 111(3), 170-174
- 671 Parlange, J. Y. (1972), Theory of Water Movement in Soils .6. Effect of Water Depth over Soil,
672 *Soil Science*, 113(5), 308-312
- 673 Parlange, J. Y. (1975), Note on Green and Ampt Equation, *Soil Science*, 119(6), 466-467
- 674 Parlange, J. Y., I. Lisle, and R. D. Braddock (1982), The Three-Parameter Infiltration Equation,
675 *Soil Science*, 133(6), 337-341
- 676 Philip, J. R. (1957a), The Theory of Infiltration: 1. the Infiltration Equation and Its Solution, *Soil*
677 *Science*, 83(5), 345-358
- 678 Philip, J. R. (1957b), The Theory of Infiltration: 4. Sorptivity and Algebraic Infiltration
679 Equations, *Soil Science*, 84(3), 257-264
- 680 Philip, J. R. (1958a), The Theory of Infiltration: 7, *Soil Science*, 85(6), 333-337
- 681 Philip, J. R. (1958b), The Theory of Infiltration: 6 Effect of Water Depth Over Soil, *Soil Science*,
682 85(5), 278-286
- 683 Philip, J. R. (1969), Theory of Infiltration, *Adv. Hydrosci*, 5, 215-296
- 684 Philip, J. R. (1973), On solving the unsaturated flow equation: 1. The flux-concentration relation,
685 *Soil Science*, 116(5), 328-335
- 686 Rahmati, M., M. Rezaei, L. Lassabatere, R. Morbidelli, and H. Vereecken (2021), Simplified
687 characteristic time method for accurate estimation of the soil hydraulic parameters from one-
688 dimensional infiltration experiments, *Vadose Zone J.*, 20. doi:10.1002/vzj2.20117
- 689 Richards, L. A. (1931), Capillary conduction of liquids through porous mediums, *Physics*, 1,

690 318-333. doi:10.1063/1.1745010

691 R Core Team (2021). R: A language and environment for statistical computing. R Foundation for
692 Statistical Computing, Vienna, Austria. URL <https://www.R-project.org/>.

693 Selker, J. S., and S. Assouline (2017), An explicit, parsimonious, and accurate estimate for
694 ponded infiltration into soils using the Green and Ampt approach, *Water Resources*
695 *Research*, 53(8), 7481-7487. doi:10.1002/2017wr021020

696 Šimůnek, J., M. T. van Genuchten, and M. Šejna (2005), The HYDRUS-1D Software Package
697 for Simulating the Movement of Water, Heat, and Multiple Solutes in Variably Saturated
698 Media, in *HYDRUS Software Series 1*, edited, Department of Environmental
699 Sciences, University of California Riverside, Riverside, California, USA.

700 Stewart, R. D. (2019), A Generalized Analytical Solution for Preferential Infiltration and
701 Wetting, *Vadose Zone J.*, 18(1), 180148. doi:10.2136/vzj2018.08.0148

702 Stewart, R. D., D. E. Rupp, M. R. Abou Najm, and J. S. Selker (2013), Modeling effect of initial
703 soil moisture on sorptivity and infiltration, *Water Resources Research*, 49(10), 7037-7047.
704 doi:10.1002/Wrcr.20508

705 Su, L., X. Yang, Q. Wang, X. Qin, B. Zhou, and Y. Shan (2018), Functional Extremum Solution
706 and Parameter Estimation for One-Dimensional Vertical Infiltration using the Brooks–Corey
707 Model, *Soil Science Society of America Journal*, 82(6), 1319-1332.
708 doi:10.2136/sssaj2018.01.0016

709 Swartzendruber, D. (1987), A quasi-solution of richards equation for the downward infiltration of
710 water into soil, *Water Resources Research*, 23(5), 809-817. doi:10.1029/WR023i005p00809

711 Talsma, T., and J. Y. Parlange (1972), One-Dimensional Vertical Infiltration, *Australian Journal*
712 *of Soil Research*, 10(2), 143-150. doi:10.1071/Sr9720143

- 713 Touma, J., M. Voltz, and J. Albergel (2007), Determining soil saturated hydraulic conductivity
714 and sorptivity from single ring infiltration tests, *European Journal of Soil Science*, 58(1),
715 229-238. doi:10.1111/j.1365-2389.2006.00830.x
- 716 Valiantzas, J. D. (2010), New linearized two-parameter infiltration equation for direct
717 determination of conductivity and sorptivity, *Journal of Hydrology*, 384(1-2), 1-13.
718 doi:10.1016/j.jhydrol.2009.12.049
- 719 van Genuchten, M. T. (1980), A closed-form equation for predicting the hydraulic conductivity
720 of unsaturated soils, *Soil Science Society of America Journal*, 44(5), 892-898.
721 doi:10.2136/sssaj1980.03615995004400050002x
- 722 Vauclin, M., and R. Haverkamp (1985), Solutions quasi analytiques de l'équation d'absorption de
723 l'eau par les sols non saturés. I. - Analyse critique *Agronomie*, 5(7), 597-606
- 724 Vereecken, H., et al. (2022), Soil hydrology in the Earth system, *Nature Reviews Earth &*
725 *Environment*. doi:10.1038/s43017-022-00324-6
- 726 White, I. (1979), Measured and Approximate Flux-Concentration Relations for Absorption of
727 Water by Soil, *Soil Science Society of America Journal*, 43(6), 1074-1080.
728 doi:10.2136/sssaj1979.03615995004300060003x
- 729 Wu, S. B., T. F. M. Chui, and L. Chen (2021), Modeling slope rainfall-infiltration-runoff process
730 with shallow water table during complex rainfall patterns, *Journal of Hydrology*, 599.
731 doi:10.1016/j.jhydrol.2021.126458
- 732 Wu, S. C., D. H. Ma, Z. P. Liu, J. B. Zhang, L. Chen, X. C. Pan, and L. H. Chen (2022), An
733 approximate solution to one-dimensional upward infiltration in soils for a rapid estimation of
734 soil hydraulic properties, *Journal of Hydrology*, 612, 128188.
735 doi:10.1016/j.jhydrol.2022.128188

